The experimental study of the coherent structures generated in the agitated vessels and effected by fluid viscosity

D. Jasikova, B. Kysela, M. Kotek, and V. Kopecky

Abstract— This paper presents results and interpretation of the dataset processed with Proper Orthogonal Decomposition (POD). The object of this work was the description of the coherent structures that are present in the mixing process. The results obtained by TR PIV measurements focused on detailed flow analysis in selected region in the context of impeller movement were processed with POD and OPD algorithms. The study was focused on the viscosity effect on the coherent structure behavior. Here we worked with three degree of viscos liquids: pure water, solution of 28% mono-ethylene glycol (MEG) and 43% MEG in water. The rounds of the Rushton impeller were set to follow the Re = (5.104 – 1.105) to perform fully turbulent flow. The main aim of this study was to analyze the coherent structures in the higher eigenmodes and its energy contribution to the flow system.

Keywords— Agitated Vessels, Oscillating Pattern Decomposition, Proper Orthogonal Decomposition, Time-resolved PIV.

I. INTRODUCTION

MIXING is a very important operation in chemical industry and process engineering because it represents more than sixty percent of all processes. Huge amount of mass is mixed in vessels stirred by an impeller. Large agitated tanks with impellers are also used in mining industry, waste water treatment, etc. In all of the above mentioned industries, the development of new technologies requires higher quality of products with lower energy demands during the product treatment. Hence, the trend is to develop more efficient mixing equipment where better knowledge of hydrodynamics is essential. Therefore, the original empirical data from basic experiments are replaced by more sophisticated numerical simulations and complex models that are continuously improved and validated by experiments [1, 2].

The knowledge of the flow inside the agitated vessel is also the background for better understanding of mixing processes, scale-up modelling, geometry improvement, etc. The results of the CFD (Computational Fluid Dynamics) based on the RANS (Reynolds Averaged Navier Stokes) approach were formerly validated by the mean values obtained by LDA (Laser Doppler Anemometry) [3] or PIV (Particle Image Velocimetry) measurements. The fast improvement in the CFD requires higher quality of the measured data. For the successful validation we should reach the highest resolution in time and space to cover the needs of the LES (Large Eddy Simulation) [4, 5, 6, 7, 8, 9, 10] and the DNS (Direct Numerical Simulation) approach [4].

The main part of published results in CFD development requirements is summarized in [11, 12]. For this reason TR PIV (Time Resolved Particle Image Velocimetry) method seems to be fine instrument that allows detailed flow analysis [13]. The PIV measurements have been used by many investigators e.g. [14, 15, 16, and 17]. In most of these experiments, the cylindrical vessel with standard Rushton impeller was used e.g. [13, 14], and [17]. The same trend follows also CFD [12], therefore the similar equipment with standard Rushton impeller for basic experimental data comparison has been chosen.

So far many experiments were run with working liquid – pure water, but on the behavior of the structures in turbulent flow has the dominant effect increasing viscosity.

The TR PIV technique brings a novel view on the data processing but also comes with complex statistical interpretation. The frequency information on the flow process and its changes can be statistically analyzed by Proper Orthogonal Decomposition – POD. The existence of traveling coherent structures and its stability can be studied with Oscillating Pattern Decomposition – OPD. The most important information while dealing with coherent structures is the kinetic energy that is captured in energetic modes. These energetic modes can be calculated by the Proper Orthogonal Decomposition and Bi-Orthogonal Decomposition known as POD and BOD algorithm [18, 19, and 20].

The BOD method gives us information about time and frequency relation in time (Chronos) and space (Topos) domains. The OPD gives us complex knowledge about the flow dynamic behavior and its interactions. Frequency of typically ascending run is a sorting parameter that is good to know before detailed study. E-fold time of descending run gives the mode importance in the meaning of its higher

D. Jasikova is with the Institute for Nanomaterials, Advanced Technologies and Innovation , Technical University of Liberec, Studentska 1402/2, Liberec 1, Czech Republic, (e-mail: darina.jasikova@tul.cz).

B. Kysela, is with the the Academy of Sciences of the Czech Republic, Czech Republic (e-mail: kysela@ih.cas.cz).

probability of the given mode occurring in the flow.

In this article we use the mentioned methods on the data evaluation and comparison taken in investigated area close to the blades where the development of vortex structures source is supposed.

II. EXPERIMENTAL SETUP

A. Mixing vessel setup

Measurement of the velocity field was realized in a pilot plant flat bottomed mixing vessel with four baffles at its wall (see Fig. 1). The standard Rushton turbine impeller was used for the investigation (see Fig. 2).
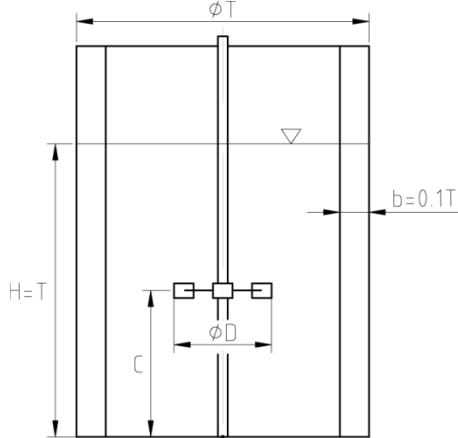
Fig. 1 mixing vessel setup (H/T = 1; D/T = 1/3; C/T = 1/2; b/T = 1/10; four baffles) impeller speed from 300 rpm to 600rpm and the position of the investigated areas

The liquid flow generated just below the impeller blade was in the scope of the interest so the middle of the investigated area was centered in the axis of the blade in the distance 50mm below the blade's edge.

The basic measurement and the coherent structure visualization were done with the water as the working liquid (density ρ = 1000 kg.m^3, dynamic viscosity μ = 1 mPa.s). The impellers rounds were set to follow the Reynolds number that is mentioned in the table 1.

For the study of liquid behavior under different viscosity we have chosen mono-ethylene-glycol (MEG) solutions. The two solutions were prepared: one with the concentration 28% of pure MEG in water with kinematic viscosity 2.03 m^2/s and 43% MEG with density 1064 kg/m^3 and kinematic viscosity 3.04 m^2/s. at 20°C.

Investigations were performed in fully turbulent regime where the mixing Reynolds number is high enough (ReM > 104), and the power number of impeller become independent on Reynolds number. Moreover, the mean flow field is only dependent on the impeller tip speed for similar geometry

$$Re_M = \frac{n\,D^2\rho}{\mu} \qquad (1)$$

Where n are impeller speed, D impeller diameter, ρ operating liquid density and μ dynamic viscosity.
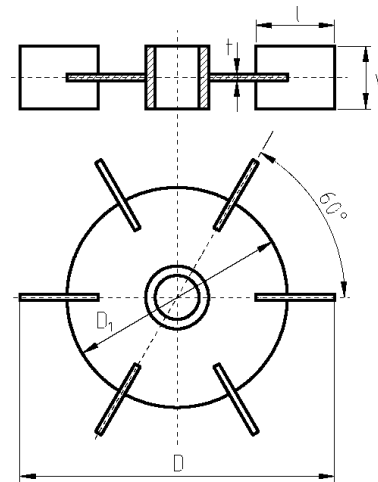
Fig. 2 standard Rushton turbine impeller (w/D = 1/5; D1/D = 3/4; l/D = 1/4; t/D = 1/50; six blades)

Table 1. Experimental impeller speeds.

Impeller speed in water [rpm]	Reynolds number
300	$5.0 \cdot 10^4$
450	$7.5 \cdot 10^4$
600	$1.0 \cdot 10^5$

During the measurement with viscous liquids the impeller speed was optimized to keep the selected Re number.

B. Measurement technique

The investigated area in the mixing vessel was examined by the time-resolved PIV technique. This measurement technique enables to measure highly turbulent flow and the development of turbulent structures over the whole investigated area. The resolution of the method depends on the setup of dynamic range. The supposed velocity range was up to 5m/s so the time between pulses was adjusted to this flow velocity. We expected the fluid flow deceleration in the steady part of the flow. So the setup of dynamic range was taken into account so the final measurement accuracy entered the 5%.

Here we used DantecDynamic TR-PIV setup that consists of the Litron LD: Y300 laser operation on the frequency 1kHz. This kind of double cavity laser emits pulses of energy reaching 15mJ in each pulse on wavelength 527nm. The laser beam was extended into the vertical plane with cylindrical optics to reach the parameter of the planar laser sheet of thickness 1mm and spread into the 100mm width.

The working liquid was seeded with 20um fluorescent particles labeled with Rhodamine B emitting on the wavelength 570nm.

The high speed camera SpeedSense working on frequency 1kHz with resolution of (1280x800)px in double frame mode was equipped with low-passing filter to eliminated the backward flashes from the laser sheet that arises on the blades surfaces. The wavelength of the optical filter corresponds with the emitted light of the fluorescent particles.

The camera was mounted with optical lens system Nikkon

Macro 200 to get detailed image of magnification 1:1 in the distance 700mm far from the blade central axis.

The laser and camera system was synchronized via timer box and controlled from the DantecStudio software. The dataset of 5000 images was captured in one run. The raw images were also processed in this software.

As the glass cylindrical body of the mixing vessel was closed in the glass square box and the space between both walls was filled with water, the captured pictures were distort by the different index of refraction of each phase (liquid and solid). Here should be mentioned that the diffractive index of water and MEG solution differs. The diffractive index of water is 1.33, for MEG 28 it is 1.37, MEG 43 it is 1.39 and the glass 1.42. This physical parameter also play substantial role in the image reconstruction.

Due this complication the pictures had to be pre-processed by the dewarping algorithm and masking function. The PIV analysis run under standard cross-correlation method with interrogation area size (32x32) pix and overlap 50%.

The raw vector maps were validated with peak and range validation methods to obtain correct dataset. For the purpose of overview of the complex flow behavior, the statistical evaluation and the turbulence index were calculated.

The dynamically changing velocity field was analyzed by the Proper Orthogonal Decomposition (POD) for identifying the energy fractions. The probability of the structures were calculated with the help of Bi-Orthogonal Decomposition (BOD) and OPD algorithm and taken into relation with stirrer's rounds setup.

III. RESULTS AND DISCUSSION

There was expected upward fluid flow in the selected area. This flow was assumed to be directed toward impeller blades.

Although relatively streamlined flow without obvious vortex structures was assumed; this flow is unsteady and on sampling frequency 1 kHz highly variable. In previous statistical measurements that were done with conventional PIV on 16Hz frequency, these rapid changes were elusive.

The relationship between the impeller rounds and flow rate in the second region corresponds to an ascending velocities of both the input and output flow. The input statistical velocity field of the flow in the second region is varying in the velocity maximum, thus the scaling is modified for each statistics, unlike as it is interpreted in Fig. 3. During the evaluation of statistical data we have used the different scales due to the visibility and highlight of any changes (Fig. 5).

Figure 3 shows the mean flow field and the pictures show the scalar field filled with the streamlines of the main averaged water flow. This statistics were obtained from the datasets of 5000 pictures and here the impact of each one vortex structure presence is suppressed. The meaning of the flow field statistics is in the description of the velocity distribution, the stream acceleration and its main tendency.

The presence of vortex structures takes shape in the statistics of the intensity of turbulence {UV}. From the figure 4 it is obvious that bellow the center line of the propellers blade the massive vortex structures is developed and this non-

stationary structure moves in vertical plane towards the main flow stream. These turbulent structures are one of the important part for the calculation of the complex kinetic energy of the whole field as well as the mean velocity part.

a)
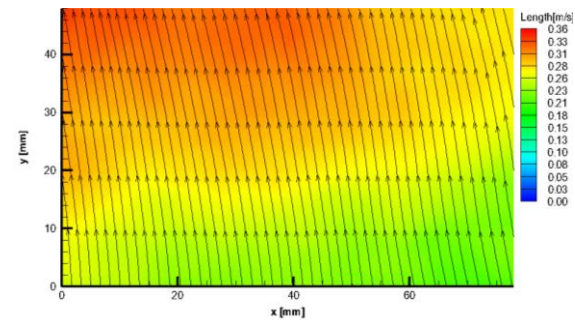
b)
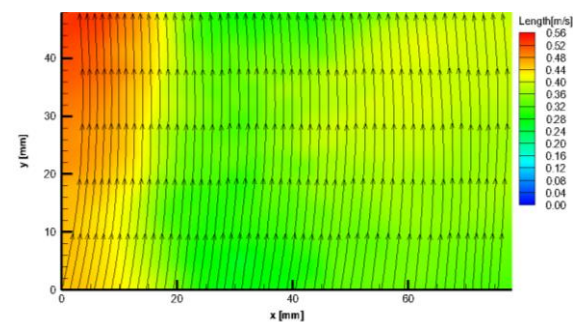
c)
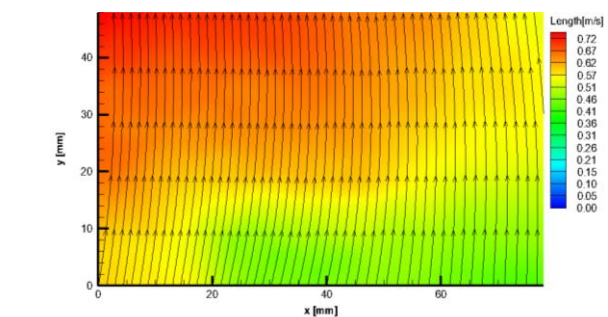
Fig. 3 the statistics of the velocity flow field (medium – pure water) for a) 300rpm, b) 450 rpm and c) 600rpm of the impeller

The figure 4 shows the most dominant vortex structure arisen in regime 450rpm and the maximum of turbulence intensity are concentrated into the area that corresponds with the main stream acceleration. The vortex structures here are significantly higher in correlation to 300rpm and 600rpm. In these regimes the intensity of turbulence is spread into the whole area and the vortex structures are larger (600rpm) and on the other hand the maximum speed is lower and the vortex is strictly located and collapse after 8ms and coalesces with the main stream. In the regime 450rpm the vortex structure can be identified in the main stream over the whole width of investigated area (more than 20ms).

a)

b)

c)
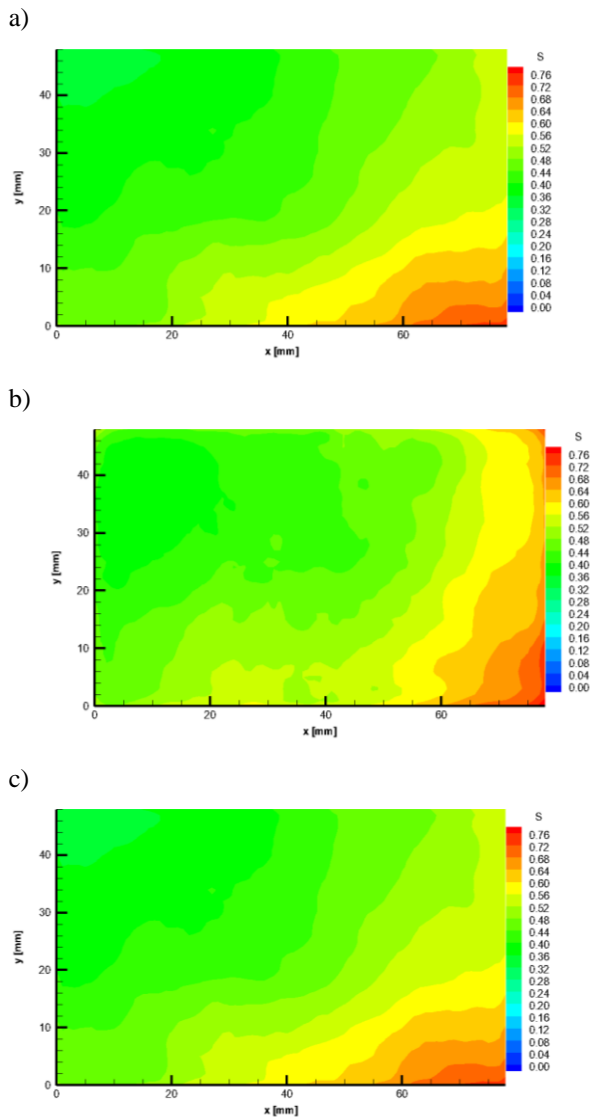
Fig. 4 the statistical results of turbulence intensity {UV} (medium – pure water) for a) 300rpm, b) 450rpm and c) 600rpm

This existence of coherent structures in the central vertical axis of the agitated vessel just below the propeller was further studied with TR PIV to get the complex view on the kinetic energy and the structures characteristics.

Here we present the reconstruction by POD modes for the eigenmodes 1, 5 and 10 that shows the most energy contribution to the flow in the selected investigated area. The figure 5 shows the selected eigenmodes and the fluid flow for the water. Here the eigenmode 0 represents the statistic value over the all processed dataset with the highest energy contribution. The velocity of the following coherent structures is one order less than the mean flow value.

a)

b)

c)
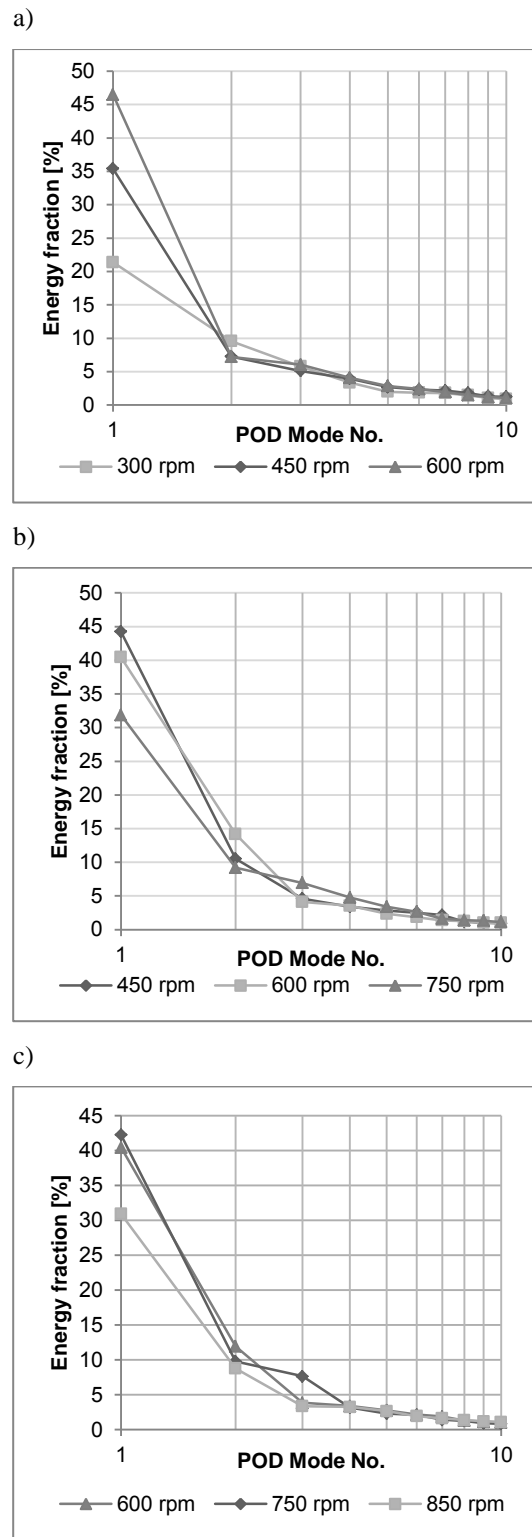
Fig. 6 the Energy fractions on the POD mode numbers for the working liquid: a) water, b) MEG 28% and c) MEG 48%

The Fig. 6 shows the relative contribution of individual POD modes for each rotation setup. There can be seen different distribution of energy for 300rpm and 600rpm of the selected 3 modes (Fig. 5). The dependence of the kinetic energy on the rounds and the rest of the curve indicate the

Mode No 1   Mode No 5   Mode No 10

300 rpm

450 rpm

600 rpm

Fig. 5 POD interpretation of the coherent structures in the water flow for a) 300rpm, b) 450rpm and c) 600rpm

same characteristics. The zero POD mode of the flow contains 46.5% of energy for 600rpm but 21% for 300rpm this shows that in the rotation 600rpm more kinetic energy is carried by the vortex structures in the second and higher modes; compared to 450rpm the difference is for the first POD mode 7% (600rpm) and (450rpm) but 9% (300rpm) and for the third POD mode is the situation almost the same and the energy contribution for all there rotational setup is round 6%.

The most significant difference in the POD modes and the vortex structures can be seen between 300rpm and 600rpm as it is seen on the figure 6. Although the dataset was processed in the 1000 eigenmode to get the complete characteristic of the energy contributions, here we present only first 10 modes to uncover single contribution of each mode.

The amount of energy obtained in the first five modes indicates the level of coherency that is present in the flow. This means that the more kinetic energy is presented in certain modes, the more coherency structures exist in the flow and less energy participates on the noise (Fig. 5). From the POD analysis it is obvious which vortex structures are dominant in the flow and that the energy spectrum is directly related to the turbulent kinetic energy.

For the higher viscous flow the situation of the energy contribution is changed due the non-Newtonian character of liquid behavior.

Here we worked with MEG-water solution under concentration 28% and 43%. The liquid in the vessel was changed just leaving the previous visualization setup that

required a novel space and refraction index calibration.

The figure 6 shows the complex POD energy contribution of the investigated liquids. There is obvious that the changes in the viscosity reflect the changes in the coherent structure behavior.

The most energetic structure is found in the dataset in the mode no. 0.

Figure 7 shows how the MEG 28% POD Modes. In comparison to the water flow behavior, here appear more complex 3D structures in higher energy contributions. Comparing the same Re number, the first eigenmode exhibits the 15% of energy and the higher rpm of impeller round 10% of energy fractions. This behavior also corresponds with the temporary statistics of turbulence intensity – for the 300rpm the most vortex structure is presented and the extremes in the velocity changes are increased; for 450rpm the statistical analysis leads to the maximal intensity of turbulence {UV} (Fig. 4). The main vortex structures presence in Mode No. 5

and higher and for 450rpm the frequency of the vortex structure occurrence is high enough to join the structures together – this behavior is reflected in the suppression of the kinetic energy of each vortex structure. The POD analysis also reflects the lifespan of the single vortex structure and its spatial position.

The vortex structure that is moving in the vertical axis towards the impeller blade is occurring in the regime of 450rpm and 600rpm. Round this structure the flow stream is also the most accelerated and these results correspond with the temporary statistics of flow velocities but as this structures shows dominant behavior and acceleration in the z-direction, the figure 7 shows how the flow is stopped in the middle of the dominant vortex structure.

Anyway, bellow this most dominant structure that is in the focus of most researchers, there are the secondary swirling structures hidden in the further modes. These structures are moving across the area and are influenced by the main stream.
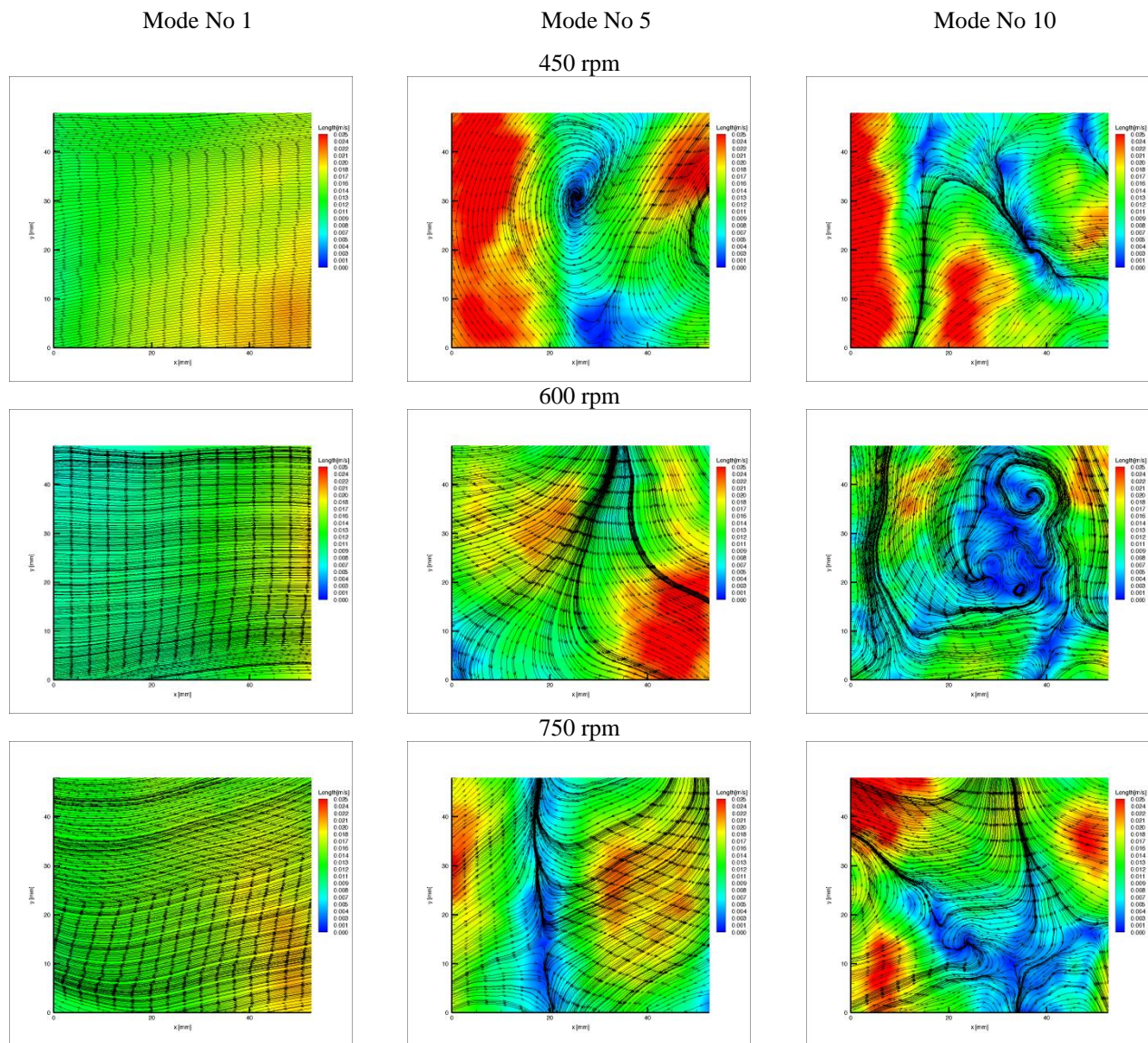
Fig. 7 POD interpretation of the coherent structures in the MEG 28% flow for a) 450rpm, b) 600rpm and c) 750rpm

As these structures take place in the sixth and higher modes, their energy contribution is about 3%. Even though the importance of these energy modes is lower, they cannot be neglected in the frequency studies and complex evaluation of TKE in the system.

On figure 7 the selected POD modes uncover the coherent structures that influencing the intensity of turbulence {UV}. Comparing the results of scalar maps it is obvious that this energy is not varying significantly according to the rounds rate.

From the statistical point of view the input seems to be stabilized with continuous streamlines and acceleration but the detailed study with TR PIV reveals the presence of complex structures.

Although the statistics of flow velocities below the impeller blade shows the uniform behavior, the intensity of turbulence {UV} uncovers the probability of vortex structures occurrence close to the central axis of the impeller. For this reason the second area was also evaluated on the POD and OPD modes

to discover the relevance of single energy fraction and probability of vortex structure.

In this investigated area it was supposed to observe the effect of secondary flow loop without any complex structures. It was studied to prove the stable character of the flow. The analysis of PIV results in this section confirmed the dependence of the flow speed on the rounds of the impeller that takes here more effect than in other areas of the primary flow loop. The higher speed of the impeller is also increasing the turbulence intensity in this area, particularly in the area round the central axis of the impeller.

The figure 7 and 8 show the POD modes for viscous fluids: MEG 28% and MEG 43% in water, the most energy contributes is in the first mode. The first mode contains the uniform flow distribution over the whole investigated area. The second mode with energy round 10% for all three regime of round brings the increase of the flow from the central axis in the opposite sense of the dominant flow. This effect is stronger in the fifth and higher mode with energy contributes

Mode No 1	Mode No 5	Mode No 10
	600 rpm	
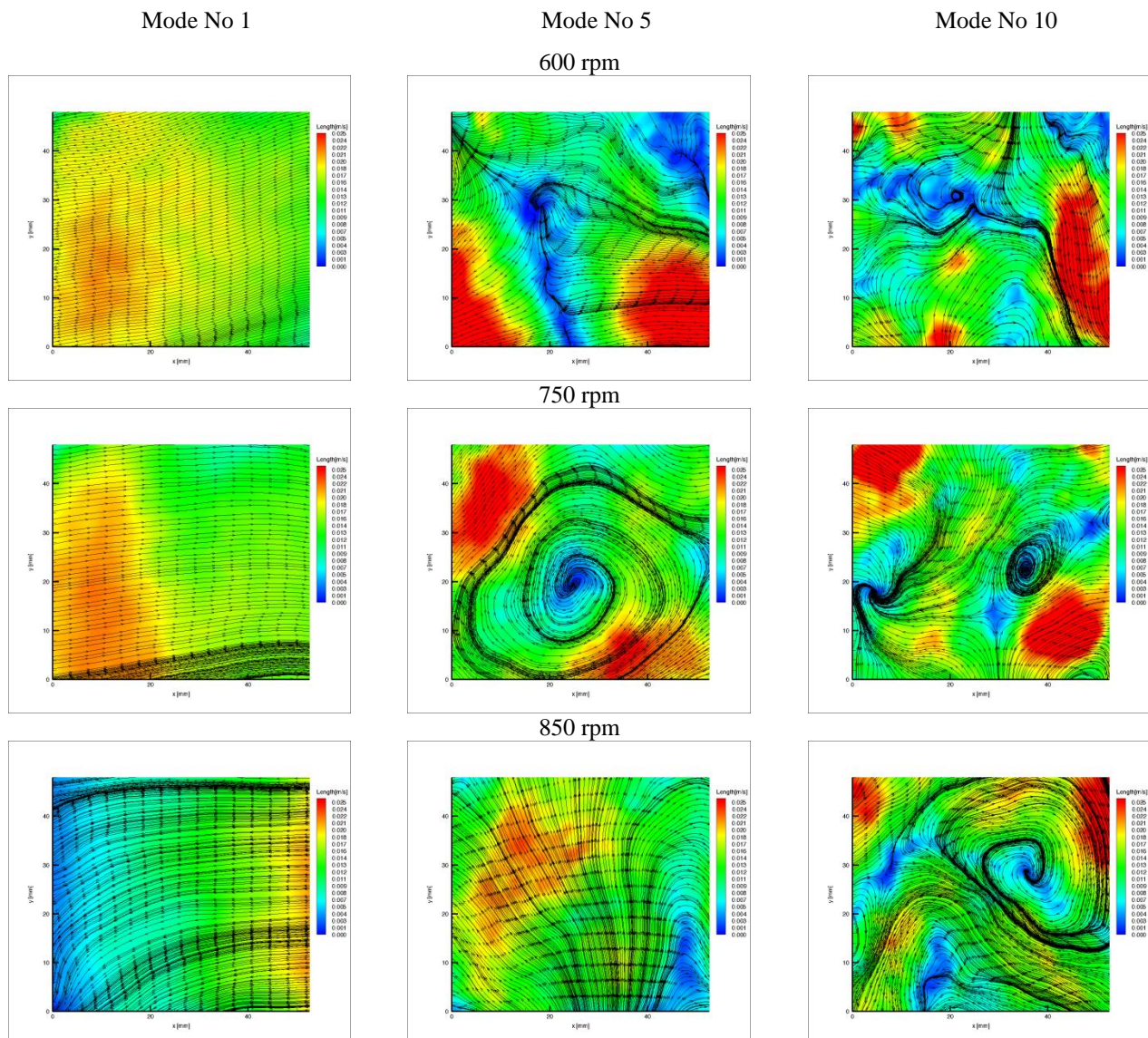
Fig. 8 POD interpretation of the coherent structures in the MEG 43% flow for a) 600rpm, b) 750rpm and c) 850rpm

round 5%.

The coherent structures that appear in the second and higher modes are responsible for the first 3D behaviour of the fluid flow. The flow in z direction is further increased with the impeller's movement. This third velocity component should undergo the detailed study, because this particular structure is affecting further behaviour of the flow behind the impeller blades, where the flow is more accelerated, even more if the coherent structure exhibits the negative character to the direction of the rotary motion.

The part of the field where the liquid is mostly accelerated corresponds with the statistical results (Fig. 3) as well as the turbulence intensity {UV} (Fig. 4), anyway the detailed character of the structures that causes this acceleration was so far uncertain. The TR measurement and POD processing brought us some suggestion and mark the direction of the further experimental work.

IV. Conclusion

Here we used the time resolved technique for the experimental study of the flow field in the agitated vessel. The results of the application POD and ODP algorithm on the captured datasets uncovered the existence of unsteady structures in the area that was assumed to be stable. The existence of these structures is bringing a novel view on the mixing process.

Within this measurement technique the dominance of inner flow structures and its energy contribution on the turbulent kinetic energy was proved. As these flow structures are not limited to the 2D plane, which most of the studies were focused on, the next step in this research is to follow the newest trends in fluid dynamics using 3D TR-PIV with two synchronized high speed cameras.

References

[1] S. M. Kresta, "The flow field produced by a pitched blade turbine: Characterization of the turbulence and estimation of the dissipation rate", *Chemical Engineering Science*, 48(10), 1993, pp. 1761-1774.

[2] K. C. Lee, "Turbulence properties of the impeller stream of a Rushton turbine", *AIChE Journal*, 44(1), 1998, pp. 13-24.

[3] M. Schafer, "Detailed LDV Measurements for Visualization of the Flow Field Within a Stirred-Tank Reactor Equipped with a Rushton Turbine", *Chemical Engineering Research and Design*, 75(8), 1997, pp. 729-736.

[4] J. Derksen, "Large eddy simulations on the flow driven by a Rushton turbine", *AIChE Journal*, 45(2), 1999, pp. 209-221.

[5] I. Fort, "Flow Characteristics of Axial High Speed Impellers", *Chemical and Process Engineering*, 31(4), 2010, pp. 661-679.

[6] J. Gimbun, "Detached eddy simulation on the turbulent flow in a stirred tank", *AIChE Journal*, 58(10), 2012, pp. 3224-3241.

[7] M. Jahoda, "CFD Modelling of Liquid Homogenization in Stirred Tanks with One and Two Impellers Using Large Eddy Simulation", *Chemical Engineering Research and Design*, 85(5), 2007, pp. 616-625.

[8] B. Kysela, "CFD Simulation of the Discharge Flow from Standard Rushton Impeller", *International Journal of Chemical Engineering*, 2014, pp. 1-7.

[9] Z. Li, Y. Bao, "PIV experiments and large eddy simulations of single-loop flow fields in Rushton turbine stirred tanks", *Chemical Engineering Science*, 66(6), 2011, pp. 1219-1231.

[10] Z. Li, "Particle Image Velocimetry Experiments and Large Eddy Simulations of Merging Flow Characteristics in Dual Rushton Turbine Stirred Tanks", *Industrial & Engineering Chemistry Research*, 51(5), 2012, pp. 2438-2450.

[11] J. B. Joshi, "CFD simulation of stirred tanks: Comparison of turbulence models. Part I: Radial flow impellers", *The Canadian Journal of Chemical Engineering*, 89(1), 2011, pp. 23-82.

[12] J. B. Joshi, "CFD simulation of stirred tanks: Comparison of turbulence models (Part II: Axial flow impellers, multiple impellers and multiphase dispersions)", *The Canadian Journal of Chemical Engineering*, 89(4), 2011, p. 754-816.

[13] A. Line, "On POD analysis of PIV measurements applied to mixing in a stirred vessel with a shear thinning fluid", *Chemical Engineering Research and Design*, 91(11), 2013, pp. 2073-2083.

[14] R. Escudie, "Experimental analysis of hydrodynamics in a radially agitated tank", *AIChE Journal*, 49(3), 2003, pp. 585-603.

[15] B. Kysela, "Study of the turbulent flow structure around a standard Rushton impeller", *Chemical and Process Engineering*, 2014, pp. 137-147.

[16] J. J. J. Gillissen, "Direct numerical simulation of the turbulent flow in a baffled tank driven by a Rushton turbine", *AIChE Journal*, 58(12), 2012, pp. 3878-3890.

[17] V.V. Ranade, "Trailing Vortices of Rushton Turbine: PIV Measurements and CFD Simulations with Snapshot Approach", *Chemical Engineering Research and Design*, 79(1), 2001, pp. 3-12.

[18] B. Patte-Rouland, "3D turbulent flow field af an annular jet", *Int. journal of mechanics*, 2(6), 2012, pp. 113-120.

[19] S. Danaila, "Proper Orthogonal Decomposition Analysis for Unsteady Rotor-Stator Interaction in a Low Pressure Centrifugal Compressor", *WSEAS transactions on Fluid Mechanics*, 3(5), 2010, pp. 226-235.

[20] Z. Yang, "On coherent structures in a separated/reattached flow", *WSEAS transactions on Fluid Mechanics*, 2(3), 2008, pp. 143-153.